17th Brazilian Congress of Thermal Sciences and Engineering
November25th-28th, 2018, Águas de Lindóia, SP, Brazil

# ENCIT-2018-0406
# CFD ANALYSIS APPLIED TO WATER METERS DESIGN AND PERFORMANCE

**Brasselotti, Bruno**
**Moura, Luiz Felipe Mendes**
Universidade Estadual de Campinas, Faculdade de Engenharia Mecânica, Departamento de Engenharia Térmica e de Fluidos.
UNICAMP/FEM/DETF
Cid. Universitária
13083-970 - Campinas, SP - Brasil - Caixa-postal: 6122
bbrasselotti@gmail.com, felipe@fem.unicamp.br

***Abstract:*** *Through the 3D CAD model of a single-jet water meter, a CFD analysis was performed considering flows in laminar, transitional and turbulent regime. The studied water meter is characterized by velocimetric type, whose interaction between the turbine and the impacted jet was studied providing information of physics quantities such as: torque curves, pressure and velocity contours, pressure loss calculation, metrological error curves and angular velocity on turbine according applied flow rate. The mechanical friction between the turbine axis and the bearing is of vital importance, reflecting directly on the sensitivity at low flows rates, such phenomenon was studied and analyzed the contribution at angular velocity on turbine. The results were validated by means of experimental tests did out on test benches.*

***Keywords:*** *CFD, water meter, metrological error, pressure loss, torque.*

## 1. INTRODUCTION

Single jet water meters are widely applied in residential, commercial and industrial areas, to measure the consumption of drinking water. Considering its robust design coupled with its high sensitivity in low flow rates and its extensive measuring range, it makes an essential product for estimating water distribution losses, it helps consumers to be aware of the importance of rational water use and to avoid leaks and waste, besides having an expressive profitability for the water supply companies.

A water meter is basically a metallic or composite body, with a measuring chamber and a turbine, which it receives the impact of the water from the inlet. In theory, the angular velocity of the turbine is proportional the applied flow, in which at each a known volume is moving to outlet, this is called a cyclic volume K. However empirically the angular velocity does not converge with the theory, reflecting in a deviation between the volume registered by the water meter and the volume consumed. These deviations depend on the operating flow of the water meter, such deviations being normalized by ISO 4064/2014, in which it also denotes that the formation of the interpolated curve from the deviations as a function of the operating flow, get the error curve of the water meter. The physics on a water meter has certain complexity to be understood and measured analytically, such magnitudes are the torques and pressures exerted on turbines blades, in which they depend on the position of turbine in relation the inlet, pressure loss calculation, measure the torque which acts in the opposite direction to rotation of turbine due to drag, friction between moving components and inertial values of the components of register system, irregular geometries, in summarize are many the unknown variables and no have many studies for obtaining information inherent to the studied physics system from analytical forms.

The flow rates studied were the main required according to ISO 4064/2014 for the residential water meter class, $Q_4$, $Q_3$, $Q_Y$, $Q_X$, $Q_2$ and $Q_1$.

Table 1. Flow rates.

| Rate Flow | Q [l/h] |
|---|---|
| **Q4** | 1250 |
| **Q3** | 1000 |
| **QY** | 750 |
| **QX** | 350 |
| **Q2** | 16 |
| **Q1** | 10 |

## 2. NUMERICAL SIMULATION

The Ansys CFX 18.1 commercial package was used to obtain results in the study, this software uses the Finite Volume Method to discretization the equations that govern the physics system studied. Ansys CFX is a general purpose Computational Fluid Dynamics (CFD) software suite that combines an advanced solver with powerful preprocessing and post processing capabilities.

## 3. GOVERNING EQUATIONS

The fluid domain was extracted from the CAD geometry which comprises the internal volume of water meter in analysis, split in static domain and rotative domain.

Different forms of the Navier-Stokes equations were applied in this study, assuming the fully internal volume of the meter by water at 25°C, thus considering an incompressible fluid. The unsteady Navier-Stokes equations for laminar flows were applied, they can be written in their vector form as:

$$\nabla \times u = 0 \tag{1}$$

$$\frac{\partial u}{\partial t} + \nabla \times (uu) = -\frac{1}{\rho}\nabla\rho + \nabla \times \left[\nu\left(\nabla u + \nabla u^{T}\right)\right] \tag{2}$$

For flows with high values of Reynolds numbers, the unsteady Reynolds averaged Navier-Stokes was applied, considering the totally turbulent flow and adopting the Boussinesq hypothesis, got:

$$\nabla \times U = 0 \tag{3}$$

$$\frac{\partial U}{\partial t} + \nabla \times (UU) = -\frac{1}{\rho}\nabla P + \nabla \times \left\{(\nu + \nu_t)\left[\left(\nabla U + \nabla U^{T}\right)\right] - \frac{2}{3}kI\right\} \tag{4}$$

The turbine was considered as a rigid body, however the rotation is governed by the system of ordinary differential and can be write:

$$I_T = \frac{d\omega_T}{d_t} = T_{WJ} - T_B - T_R \tag{5}$$

Where, $I_T$ is the inertial moment of turbine, $\omega_T$ is the rotation speed and $T_{WJ}$, $T_B$ and $T_R$ the torques on system, being, $T_{WJ}$ the torque due the water jet impact each blade, $T_B$ the torque due the friction between pivot axis with the bushing and $T_R$ the torque equivalent the gears, magnetic coupling and other physics present on the register.

Basically the system works with the positive torque, formed per the driving torque $T_{WJ}$ due the water jet impacted on blades of turbine and the retarding torques, that works as negative torque, once the turbine drag the water, both torques, $T_R$ and $T_B$ are sensible magnitudes to get and measure, this torques will be conjugated in an only term and adopted different values in set up to transient analysis. This torques always will work as negative values, once that the both the torques are formed with friction mechanical contact and inertial moment.

## 4. BOUNDARY CONDITIONS

The static domain was split in segments at the regulars circle sections, being possible apply the O-grid concept to get the mesh, according figure 1. This concept to mesh generation allowed create of a structured mesh and consequently the reduction the number of elements and nodes of fluid model, established the alignment of mesh elements with the flow to avoid the numerical diffusion. For better resolution of results the developing flow and capture of wall effects, the elements were smoothly reduced until 0,04 mm in contact of wall. The mesh was discretized with 1,599,953 nodes and 4,245,101 elements, being 600,000 hexahedrons, 919,427 prisms, 4,245,101 tetrahedrons and 4,678 pyramids, about the mesh quality rating, the maximum skewness is 0.893 and orthogonal quality minimum is 0.087.

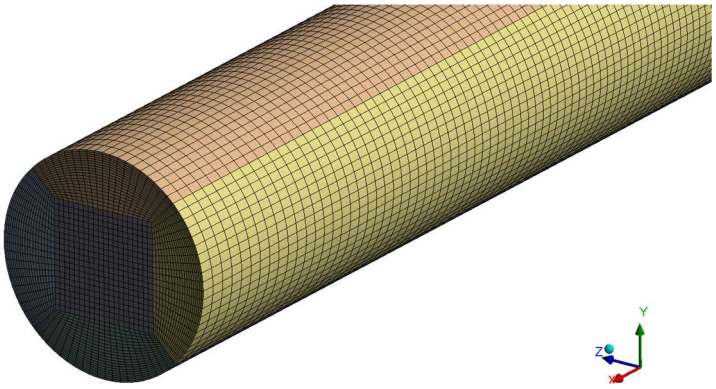


Figure 1. O-grid concept to structural mesh

The boundary conditions were applied at static and moving walls of the meter, pipes, inlet and outlet. All static and moving walls the non-slip conditions was declared. At inlet the mass flow rate was applied considering the flow profile fully developed, due the in the absence of experimental data, was adopted medium intensity to turbulence, this defines a 5% intensity and a viscosity ratio $\mu_t$ / $\mu$ equal to 10.

At outlet only the static pressure was prescribed as with zero gauge pressure, being the fluid considered incompressible, only pressure gradients are the focus. Other advantage when prescribed zero-gauge pressure in outlet is the minimize process round-off on solver step, showed figure 2.

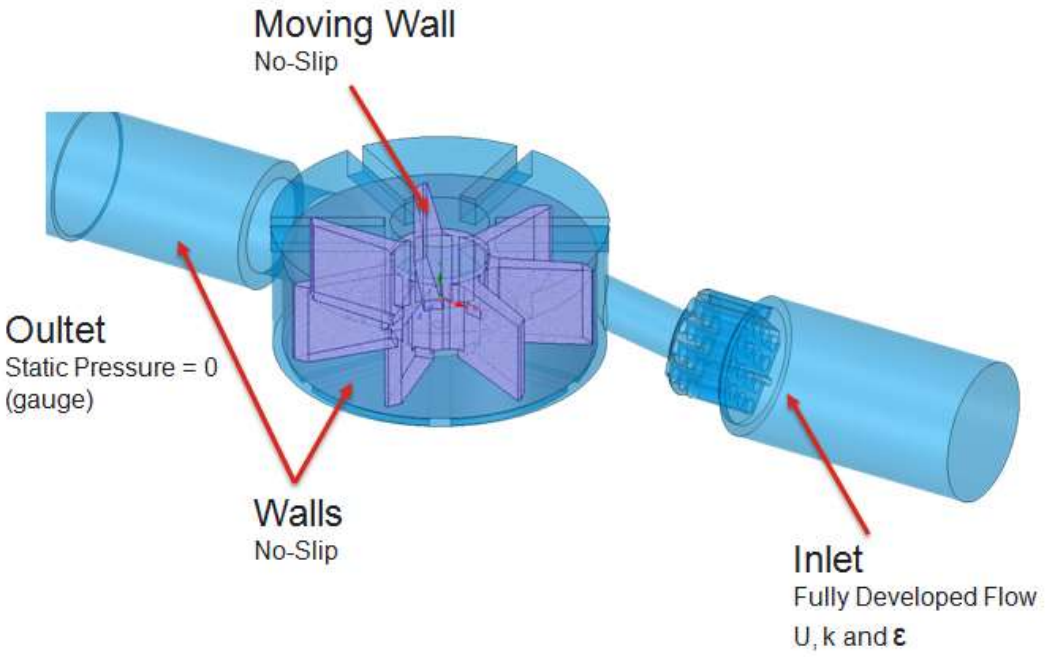


Figure 2. Fluid Domain and Boundary Conditions

According the angular velocity and consequently the Reynolds number a time discretization, time step and turbulence model was prescribed.

The theoretical angular velocity can be estimated and write as:

$$\omega T_{Theoretical} = \frac{2\pi KQ}{3600} \left[\frac{rad}{s}\right] \quad (6)$$

Where:

Q = flow rate [l/h]

$$K = \frac{1}{\mathrm{CV}}$$

CV = Cycle volume [liters / revolutions]

The Reynolds number is the ratio of the inertial forces and the viscous forces. In practice, the Reynolds number is used to predict if the flow will be laminar or turbulent.

If the inertial forces, which resist a change in velocity of an object and are the cause of the fluid movement, are dominant, the flow is turbulent. Otherwise, if the viscous forces, defined as the resistance to flow, are dominant the flow is laminar. The Reynolds number can be specified as below:

$$Re = \frac{Inertial\ force}{Viscous\ force} = \frac{VL}{\nu} = \frac{\rho VL}{\mu} \quad (7)$$

For the rotative domain, the Reynolds number is related to the circumference $Re_U$, so it can be write as:

$$Re_u = \frac{\pi n D^2}{\nu} \quad (8)$$

Where:

$D$ = turbine diameter [m]

V = characteristic velocity of the flow [m/s]

L = is the characteristic length scale of flow [m]

n = angular velocity [rps]

μ = dynamic viscosity of water [Pa.s]

ν = kinematic viscosity of water [$m^2/s$]

$\rho$ = density of water [$kg/m^3$]

For μ and ρ values was adopted the temperature being 25°C.

Table 2. General data for numerical simulation

| Rate Flow | Q [l/h] | ωT [rpm] | ωT [rps] | ωT [rad/s] | ωT [degree/s] | Reynolds Number | Time Step [s] | Number of laps | Total Time [s] |
|---|---|---|---|---|---|---|---|---|---|
| Q4 | 1250 | 1303,63 | 21,73 | 136,52 | 7821,79 | 147622 | 0,0001278 | 3 | 0,1381 |
| Q3 | 1000 | 1042,91 | 17,38 | 109,21 | 6257,43 | 118071 | 0,0001598 | 3 | 0,1726 |
| QY | 750 | 782,18 | 13,04 | 81,91 | 4693,07 | 88587 | 0,0002131 | 3 | 0,2301 |
| QX | 350 | 365,02 | 6,08 | 38,22 | 2190,10 | 41304 | 0,0004566 | 3 | 0,4931 |
| Q2 | 16 | 16,69 | 0,28 | 1,75 | 100,12 | 1902 | 0,0499406 | 3 | 10,7872 |
| Q1 | 10 | 10,43 | 0,17 | 1,09 | 62,57 | 1154 | 0,0799050 | 3 | 17,2595 |

A steady-state analysis for each flow rate was obtained initially to take approximate values, in which they were subsequently used as initial data for the transient state analysis.

The turbine was initially assembled on CAD model and kept at fluid model with one aleatory blade forming an angle of 90 degrees with the center line of inlet. In the transient solution the time step used was equivalent to 1º of rotation the turbine to flows rates $Q_4$, $Q_3$, $Q_y$ and $Q_x$ and 5º of rotation the turbine to the flows rates Q2 and Q1.

The turbine has 7 blades, in which each 51,43° a cycle of spatial positioning of the blades coincide, thus initiating a new cycle. The torque values will be captured every 10 ° of rotation of the turbine, with the initial position being equal to 0 °, sequenced at 10 °, 20 °, 30 °, 40 ° and 51,43°.

The turbulence model was applied according the Reynolds number, being applied to low Reynolds the k-ω SST turbulence model at $Q_2$ and $Q_1$ and k-ε to high Reynolds number at $Q_x$, $Q_y$, $Q_3$ and $Q_4$.

For the k-ε turbulence model the wall function is scalable scheme is used, the scalable wall functions overcome one of the major drawbacks of the standard wall function approach in that they can be applied on arbitrarily fine meshes. If the boundary layer is not fully resolved, the advantage is will be relying on the logarithmic wall function approximation to model the boundary layer without affecting the validity of the scalable wall function approach.

About the k-ω SST turbulence model used the automatic near-wall treatment, automatically switches from wall-functions to a low Reynolds number near wall formulation as the mesh is refined. One of the well known deficiencies of the k-ε model is its inability to handle low turbulent Reynolds number computations. Complex damping functions can be added to the model, as well as the requirement of highly refined near-wall grid resolution $y + < 0.2$ in an attempt to model low turbulent Reynolds number flows. This approach often leads to numerical instability. Some of these difficulties may be avoided by using the model, making it more appropriate than the model for flows requiring high near-wall resolution. However, a strict low-Reynolds number implementation of the model would also require a near wall grid resolution of at least $y + < 2$.

Monitors were created to check the stabilization solution and convergence, was checked the pressure in inlet, the torque values in each of the blades and the angular velocity of turbine, in addition the residual values of the solution in such a way to understand the convergence and to make possible adjustments during the solver step. The solution was obtained when the monitors showed stable with periodic behaviors and the residuals would reach their stated minimum values less or equal to $10^{-4}$. The total solution time to achieve convergence was equivalent to 3 complete turns of the turbine.

The runtime on solve step was approximately 60 hours to each flow rate, using processor Intel Xeon CPU E5-1620 @ 3.50GHz, 8 Logical Processors, being 4 Cores in process local and parallel.

A convergence study of meshing was performed, assumption a coarse mesh 1.5x equivalent than the original in all directions and the time step was increased 1.5x also, this result had poor quality, main in the low flow rate. Based in the experience on others similar studies, this mesh prescribed gave the confidence to do the analysis results.

## 5. EMPERIMENTAL TESTS AND MODEL VALIDATIONS

The analysis validation was performed with the comparative values between the numerically obtained and experimental results, the physics characteristics compared were the angular velocity of turbine, the pressure loss and the values related to the calibration errors.

The representative scheme at figure 3, show the calibration bench is a volumetric type, which consists of a water tank, valves, pressure and temperature sensors, an electromagnetic meter for the measurement of the operation flow in the bench and calibration tanks with a resolution of 0.005 l were used to measure the volume. The measurement uncertainty associated with the calibration bench is 0.20%.

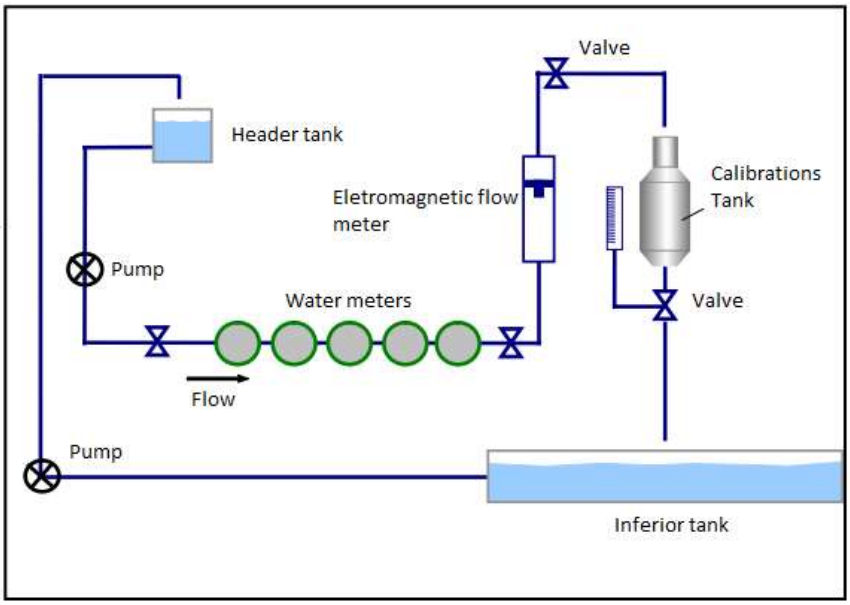


Figure 3. Draft of calibration bench

Five water meters was made and tested to get the error curve, angular velocity and pressure loss, all water meter was tested on horizontal position. The total volume drained to the calibration tanks were 100 liters for $Q_4$, $Q_3$, $Q_y$ and $Q_x$ and

20 liters $Q_2$ and $Q_1$, was performed three readings per flow rate, where the maximum deviation between readings was 0.20% to the same water meter and 0.73% between the five samples tested. The profile curve is performed with the average values of each flow rates. To get the pressure loss values, column of mercury was used in each water meter separated, the friction value between the walls pipes was not considered, once that has low roughness.

The error curve is standard according ISO 4064/2014, which are parameters used for certification and validation of water meters for residential, commercial and industrial markets, according to the regulations, the deviations must be within +/- 5% to $Q_1$ and within +/- 2% for the others ones flow rates.

The numerical validation is obtained by comparing the volume recorded by register of water meter with the amount volume on calibration tank being do the reading per an indicate

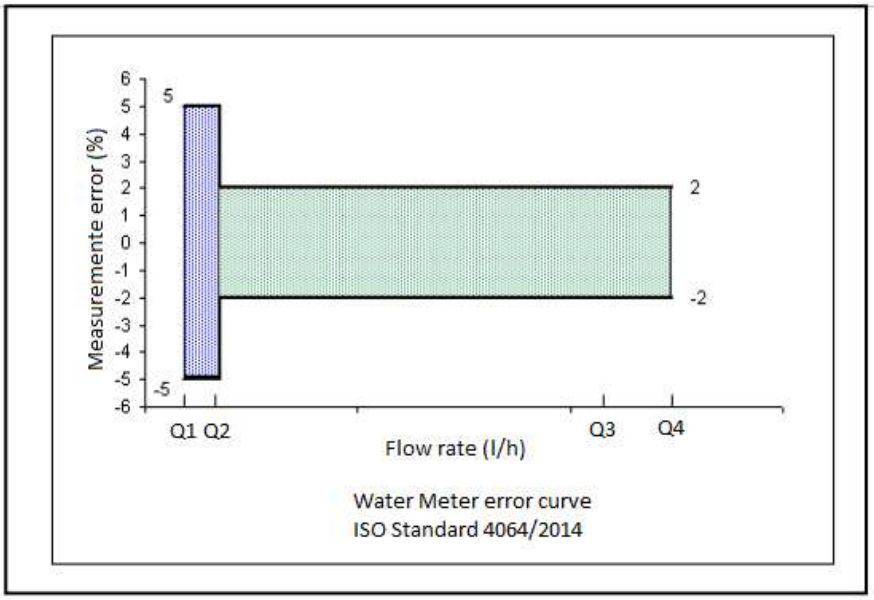


Figure 3. Scheme of the error channel

## 6. RESULTS AND DISCUSSION

The blades were numbered from 1 to 7, so that their positions were located throughout the evolution of analysis, the blade positioned perpendicular to the inlet was identified as number #1 and the other blades was subsequent the numbered counterclockwise. Velocities and pressures contours were captured in 6 distinct positions of the turbine, each position represents a rotation of 10º, getting a cycle where the rotative movement of turbine allows all the 7 blades to pass through a same reference. The velocity and pressure contours were taken in the middle plane the fluid domain, aiming at understanding the complex interaction between the turbine and the fluid, especially the interaction between jet impacted directly in the blades.

For example, the figure 4 show the study got with analysis on Q3 flow rate. The analysis showed that vane #1 has a direct influence of the jet, showed at 0º in figure 2, in which loss torque when the blade #7 cross through the inlet and starts to have the jet directly impacted in its face, showed between 10º to 30º according figure 2, this phenomenon observed at high flows causes an acceleration of the fluid near the tip of blade #7, causing a zone of low pressure in the back side, the pressure value increase gradually in the future positions in front side at blade #7.

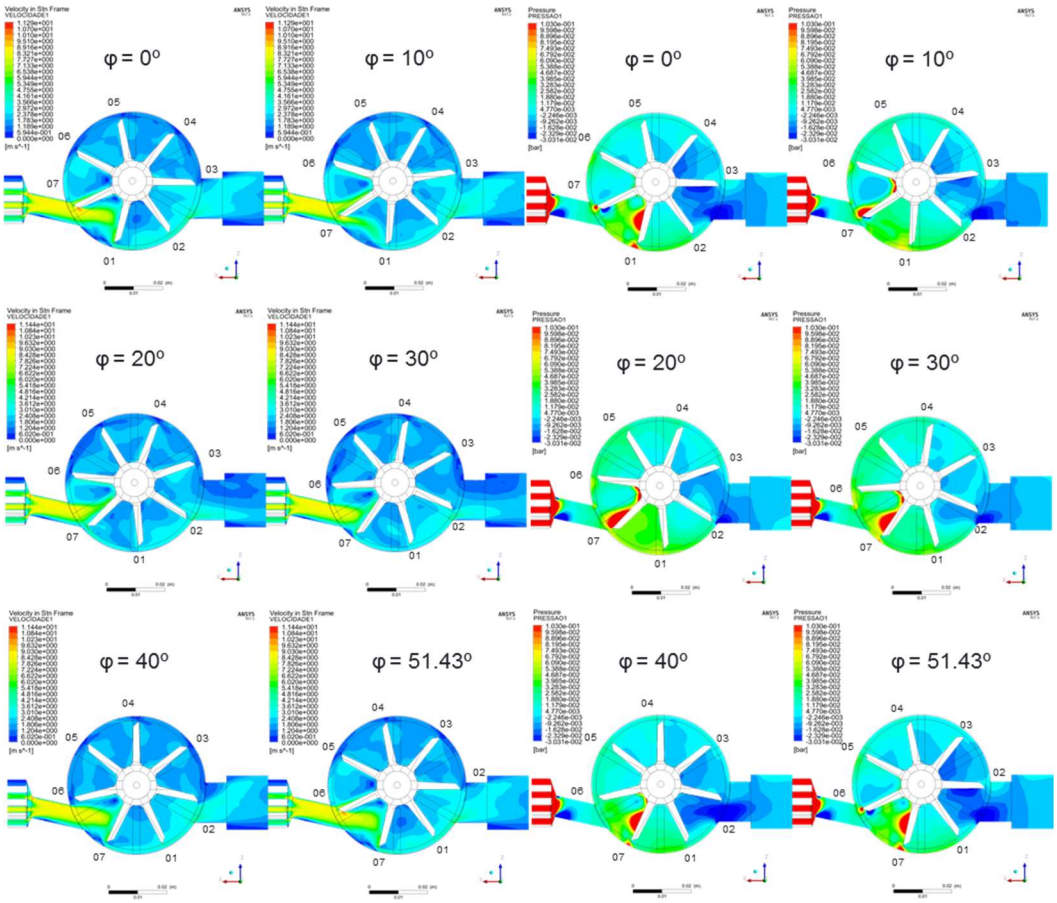


Figure 4. Velocities contours (left) and pressure contours (right) in Q3 = 1000 l / h

Another important data and observed was the oscillation of the pressure loss between the inlet and the outlet, as showed in figure 5, the pressure varies according to the turbine position, this variation is not only due to hydraulic losses, but also by the energy exchange between the turbine within the measuring chamber. As seen in figure 2, the pressure in the inlet is that it has more oscillations, since in the whole channel that comprises the outlet the pressure practically maintains constant. However, at the intersection of the measuring chamber with the start of the outlet duct, there is a region that accelerates the fluid, forming a region of low pressure.

In the empirical test this process is measured with two fixed dimensions and applied the factor to adjustment of the temperature and density of water and also the pressure loss according length of tube the device, knowing this value the value is subtracted to real calculus at inlet and outlet of water meter. In the numerical simulations is created two plans, at inlet and other one in outlet and measured the delta $P_1$ and $P_2$.

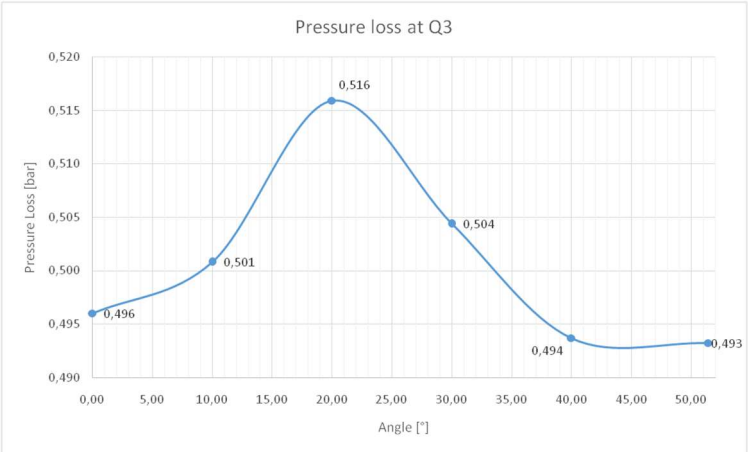


Figure 5. Pressure loss (DeltaP) at $Q_3$

In lab environment was measured the pressure loss at $Q_x$, $Q_y$, $Q_3$ and $Q_4$, the numerical results were very similar according figure 6, is possible identify a quadratic behavior, the deviation maximum was between -7% for $Q_4$ and -8% for $Q_x$. Once the mesh was kept to all flow rates, these results show the relevance of refinement mesh according the velocities fields on development flow.

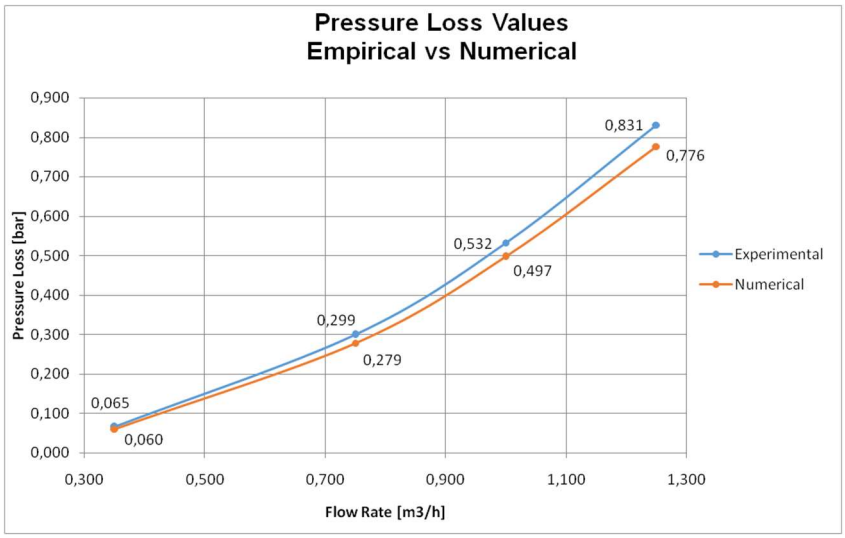


Figure 6. Pressure loss (DeltaP) at $Q_3$ = 1000 l/h

The torque got by the fluid in each of the 7 blades is showed in figure 6, it is noted torques with positive values, in this case the blade #1 and #7, which as expected, are values of torque in the blades that are under direct impact of water jet in the inlet, where the peak of the torque is approximately in 23°. The negative values of torques are found in the blades opposite to the inlet, a phenomenon explained by the drag force on the tips of blades and which acts resisting the movement of the turbine, according figure 2 in the blades #2, #3, #4, #5 and #6.

Between 10° and 20° is noted an increase on torque in blade #1, this aspect is showed according figure 4, where a high-pressure zone at back side at blade #7 and front side at blade #1 is formed. Gradually the blade #2 comes to near outlet and the contour velocities is increased and consequently a low-pressure zone is formed, clear in 30° until the final cycle.

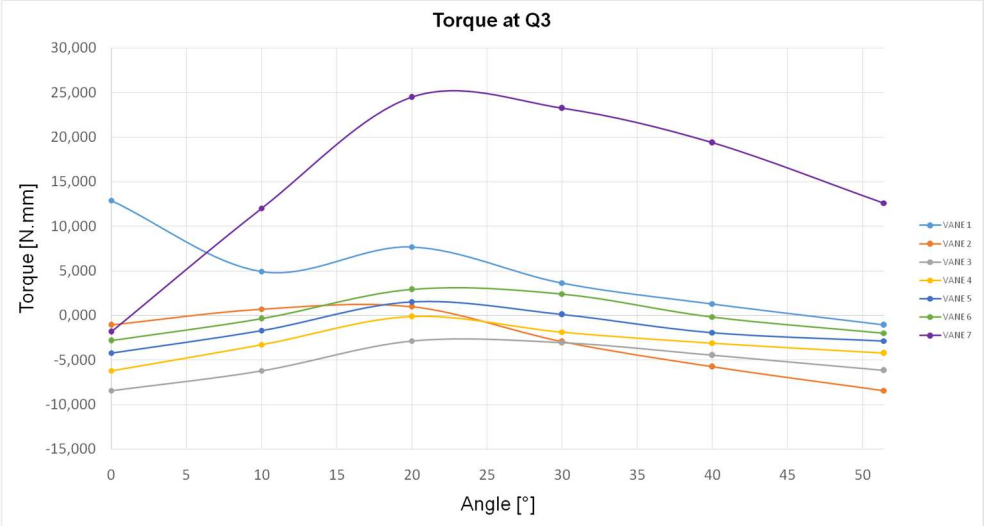


Figure 6. Torque by blade in Q3 = 1000 l / h

The torque got by each of blades is due to the pressure forces, the torques transmitted to each of the seven blades were summed and thus was the total torque produced by the flow. According the figure 7 and 8, as expected, increased the flow rate, increase the torque. The torque is the only one applied on the turbine in the simulation, the mechanical resistance in

the movement of rollers and gears of register system was not considered due to its expressive and complex it analytical to estimate its value.

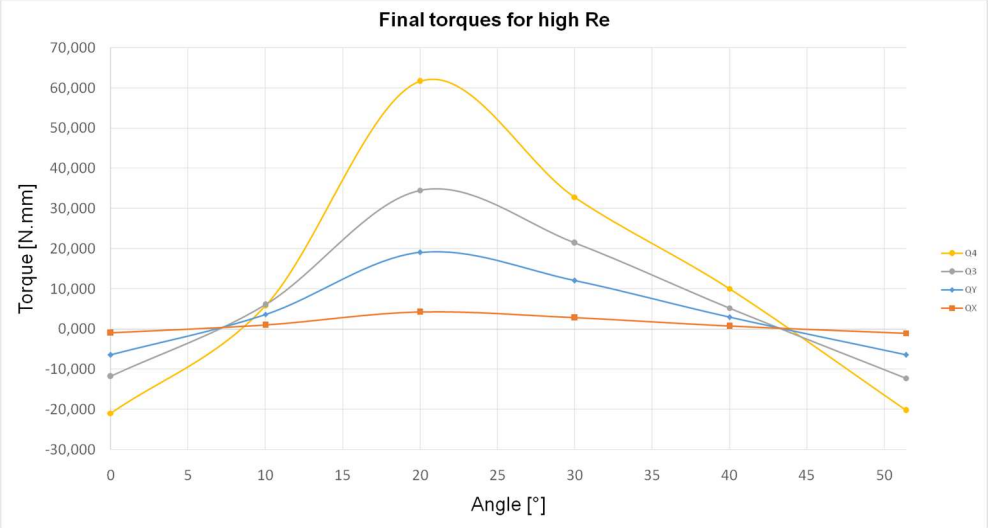


Figure 7. Torque per each flow rate with high Re

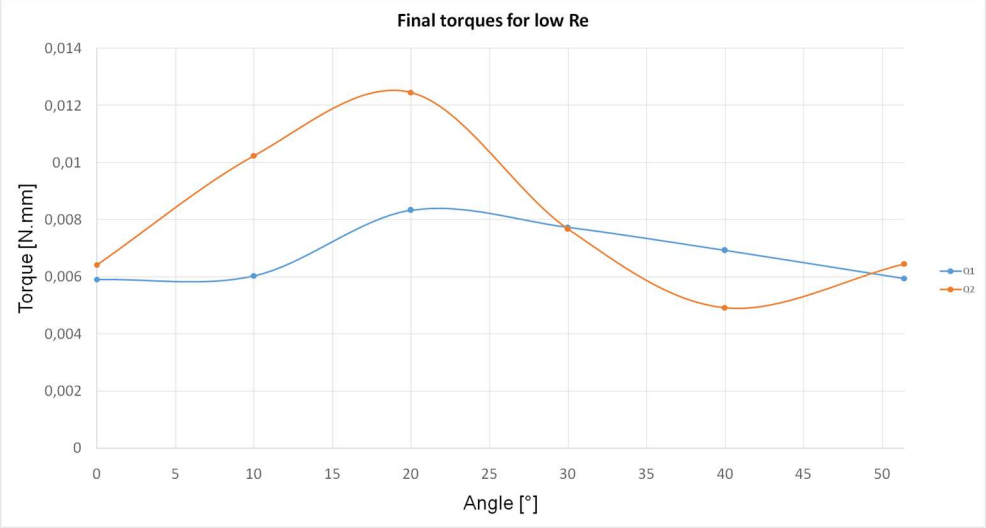


Figure 8. Torque per each flow rate with low Re

To get more accuracy and physics representation of the studied system, analyzes were performed with different values of negative torques, these torques aim to represent the mechanical resistance existing in the system, being the friction between the surfaces of the axis of the turbine with the bearing and as previously mentioned the torque values due to the inertial system of the components of the register device.

Figure 9 shows a comparison the error curves of water meter got empirically with different estimated values of negative torques got by CFD analysis, the results in showed are deviations referring to angular velocities of the turbine. The torque values were chosen in an arbitrary way but following scale a pattern magnitude.

As observed, the biggest deviations occur when the low flows rates of Q1 and Q2 are applied, in which a reduction the deviations are observed along the increasing flows rates. This same behavior is observed in the empirical tests, in which, at low flow rates, the sensitivity of the meter is significantly affected due mainly to the surface roughness and GD&T tolerances. The negative torque got the reduction at angular velocity on turbine and consequently less volume measured charged by turbine. The comparative between empirical test and numerical analysis according figure x, show that the assumptions initial about the mechanical has low influence in angular velocity can be true. Others similar studies has been the same behavior, what means, that the mechanical friction affect main the low flow rates, similar seen in empirical test.

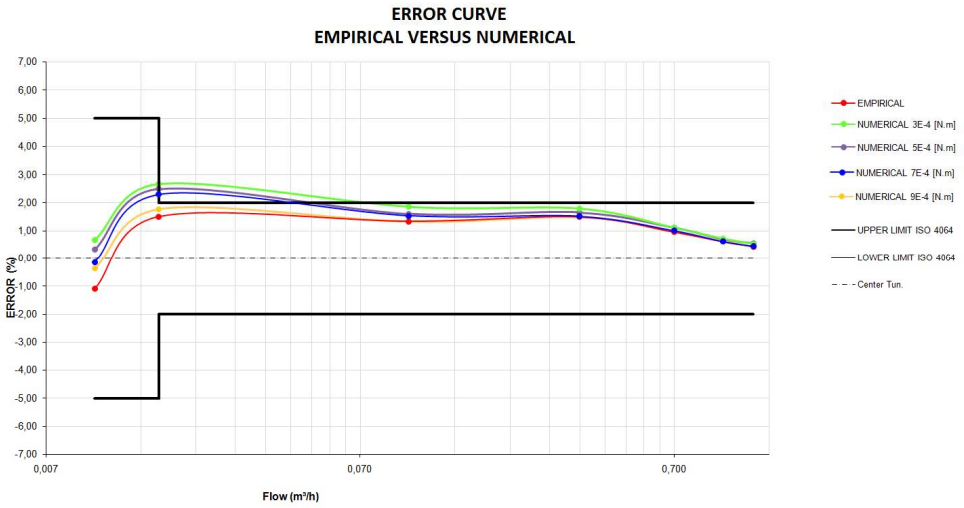


Figure 9. Error curve – empirical versus numerical simulation

The correlation between the volume measured by water meter and the angular velocity is proportional, once the water is a velocimetric type and consequently the concept is the cycle volume and angular velocity of turbine.

$$Measuring\ Error = \frac{\mathrm{Vol_{record}} - \mathrm{Vol_{real}}}{\mathrm{Vol_{real}}} = \frac{\omega T_{numerical} - \omega T_{real}}{\omega T_{real}} \quad (9)$$

## 7. CONCLUSIONS

The CFD analysis allowed got knowledge in more detail the interaction between the flow and the turbine, in which it is the main physics interaction for the prediction of performance of a water meter. In more depth it was possible analyzed and got information regarding results previously not known by empirical form. Information on turbine torques, pressure losses and the expressive possibility for innovative design with target on improving accuracy measurement on water meters.

The effect of mechanical friction was understood, especially at low flow rates, where the mathematical model reproduced with good accurately the proposed physics. The different values applied to represent the negative torque to turbine rotation showed that the velocity reduces linearly for each value applied and that the relative effect of the mechanical torque has a low influence on high flows rates, a phenomenon that is observed in the empirical analysis.

In summarize, the use of CFD applied to improvements of design and performance on water meter showed be a great tool, proving to be a powerful, versatile and vital resource to get products with more robustness, accuracy, cost reduction and saving development time.

## 8. REFERENCES

Meinecke, W., 1984. “Measuring Characteristics of Water Meters”. Aqua, 4, pp. 233-237.
Tedesco, G., 1969, “Hidrometros de Trasmissão Magnéticas”. D.A.E, 73.
Mutchnik, O., 1971, “Hidrometros”. D.A.E, 82.
Larraona, G., Rivas, A., Ramos , J.. 2008. “Computational Modeling and Simulation of a Single-Jet Water Meter”. Journal of Fluids Engineering-transactions of The Asme - J FLUID ENG. 130. 10.1115/1.2911679.
Arregui, F., Cabrera, E. J. Cobacho, R., and Garefa-Serra, J., 2005. “Key Factor Affecting Water Meter Accuracy.” Leakeage, Halifax, Canada.
Bukle, U., Durst, F., Howe, B., and Melling, A., 1992, “Investigation of a Floating Element Flowmeter”. Flow Meas. Instrum., 3, pp 215-225.
Xu, Y., 1992, “Calculation of the Flow Around Turbine Flowmeter Blades”, Flow Meas. Instrum. 3, pp 25-35.
Avraham, T., 2017. “Understanding The k-ε Turbulence Model”. 19 Mar. 2018 <https://cfdisraelblog.wordpress.com/2017/04/27/understanding-the-k-%CE%B5-turbulence-model%EF%81%A5/>.
Avraham, T., 2017. “Understanding The k-ω SST Model”. 21 Mar. 2018 < https://cfdisraelblog.wordpress.com/2017/03/23/understanding-the-k-%CF%89-sst-model/>.
Avraham, T., 2018. “Understanding the Boussinesq Hypothesis and the Eddy-Viscosity Concept”. 26 Mar. 2018 < https://cfdisraelblog.wordpress.com/2018/01/29/the-bousinesq-hypothesis-thinking-out-of-the-box/>.
Avraham, T., 2018. “Advanced ANSYS Fluent Course – Turbulence Modeling”. 22 Mar. 2018 < https://cfdisraelblog.wordpress.com/2018/03/24/advanced-ansys-fluent-course-turbulence-modeling/>.
ISO 4064-1:2014 (OIML R49), “Water meters for cold potable water and hot water -- Part 1: Metrological and technical requirements”, Standards ISO.
Ansys Engineering Simulation and 3-D Design Software, 2018,“Ansys CFX 19.1 User Help”, 15 Mar. 2018.

## 9. RESPONSIBILITY NOTICE

The authors are the only responsible for the printed material included in this paper.